

Toxicology Research

Accepted Manuscript



This is an *Accepted Manuscript*, which has been through the Royal Society of Chemistry peer review process and has been accepted for publication.

Accepted Manuscripts are published online shortly after acceptance, before technical editing, formatting and proof reading. Using this free service, authors can make their results available to the community, in citable form, before we publish the edited article. We will replace this *Accepted Manuscript* with the edited and formatted *Advance Article* as soon as it is available.

You can find more information about *Accepted Manuscripts* in the [Information for Authors](#).

Please note that technical editing may introduce minor changes to the text and/or graphics, which may alter content. The journal's standard [Terms & Conditions](#) and the [Ethical guidelines](#) still apply. In no event shall the Royal Society of Chemistry be held responsible for any errors or omissions in this *Accepted Manuscript* or any consequences arising from the use of any information it contains.

**Involvements of ROS-mediated mitochondrial dysfunction and SIRT3 down-regulation
in tris(2-chloroethyl)phosphate-induced cell cycle arrest**

Wenjuan Zhang^{1,2}, Youjian Zhang^{1,2}, Tian Xu^{1,2}, Zhiyuan Wang^{1,2}, Jing Wang^{1,2}, Wei Xiong^{1,2}, Wenhong Lu^{1,2}, Hongyan Zheng^{1,2}, Jing Yuan^{1,2*}

¹ Department of Occupational and Environmental Health, ² Key Laboratory of Environment and Health, Ministry of Education & Ministry of Environmental Protection, and State Key Laboratory of Environmental Health (Incubating), School of Public Health, Tongji Medical College, Huazhong University of Science and Technology, Wuhan 430030, Hubei, P.R.China

* Correspondence to: Prof. Jing Yuan, ¹ Department of Occupational and Environmental Health; ² Key Laboratory of Environment and Health, Ministry of Education & Ministry of Environmental Protection, and State Key Laboratory of Environmental Health (Incubating), School of Public Health, Tongji Medical College, Huazhong University of Science and Technology, Wuhan 430030, Hubei, P.R.China; Tel: +86 27 83693209; Fax: +86 27 83692701; E-mail: jyuan@tjh.tjmu.edu.cn

Abbreviations

ATP, adenosine triphosphate; DMSO, dimethyl sulfoxide; FoxO3a, forkhead box O3a; mtROS, mitochondrial reactive oxygen species; mtDNA, mitochondrial DNA; MMP, mitochondrial membrane potential; MnSOD, manganese-containing superoxide dismutase;

nDNA, nuclear DNA; PBS, phosphate buffer solution; PI, propidium iodide; ROS, reactive oxygen species; TCEP, tris(2-chloroethyl)phosphate.

Highlight

TCEP induced G2/M cell cycle arrest and mitochondrial dysfunction through enhancement of mitochondrial oxidative stress and SIRT3 down-regulation in Chang liver cells.

Abstract

Tris(2-chloroethyl)phosphate (TCEP) is a flame retardant in plastics. It is bio-accumulative and persistent in the environment and has been detected in ambient and indoor air, surface and groundwater, food, house dust, and consumer products. Studies showed that TCEP can cause damage to the liver, kidneys of rats. However, the mechanisms underlying TCEP remain unclear. To investigate effects of TCEP on the mitochondrial function and cell fate, Chang liver cells were treated with TCEP (3.12, 12.50, 50.00, and 200.00 mg/L) for 24 and 48 h. The results showed that TCEP increased mitochondrial reactive oxygen species production, disrupted mitochondrial integrity and caused mitochondrial dysfunction, representing that increased intercellular free Ca^{2+} levels, decreased mitochondrial membrane potential and mitochondrial DNA copies as well as reduced ATP synthesis, and the G2/M cell cycle arrest with down-regulations of SIRT3, forkhead box O3a and manganese superoxide dismutase proteins. The findings suggest that TCEP caused cell cycle arrest through down-regulation of SIRT3 involved in mitochondrial oxidative stress.

Keywords: tris(2-chloroethyl)phosphate; mitochondrial dysfunction; cell cycle arrest; SIRT3.

1. Introduction

Tris(2-chloroethyl)phosphate (TCEP) is used in plastics and textiles as a flame retardant plasticizer. It is ubiquitously detected in the air, water, household dust samples¹⁻⁴, as well as human hair and breast milk samples^{5,6}. TCEP is classified as carcinogenic (category 2) and toxic for reproduction (category 1B)⁷. Several *in vivo* studies have shown that TCEP was metabolized into several metabolites, including bis(2-chloroethyl) carboxymethyl phosphate, bis(2-chloroethyl) hydrogen phosphate and glucuronide of bis(2-chloroethyl) 2-hydroxyethyl phosphate in urine of rodents^{8,9}, additionally, potential linkages between TCEP and liver or kidney tumors were found in rodents^{10,11}.

Reactive oxygen species (ROS) often associated with earlier cellular events under physiological and pathological conditions¹². Several lines of evidence showed that ROS production affected cell viability and essential cellular functions^{13,14}. Mitochondria not only generate adenosine triphosphate (ATP) and maintain intracellular Ca²⁺ homeostasis¹⁵, but also are the main source of cellular ROS¹⁶. It possess a multi-leveled ROS defense network of glutathione peroxidase, manganese-containing superoxide dismutase (MnSOD)¹⁷. An imbalance between generation and removal of ROS inhibited mitochondrial Ca²⁺ accumulation can increased free cytosolic Ca²⁺ levels¹⁸, decreased ATP synthesis¹⁹, even led to cell cycle arrest and apoptosis²⁰.

SIRT3 is a mitochondrial protein deacetylase. It regulates basal ATP synthesis^{21,22}, enhanced mitochondrial anti-oxidative defense²³ and thereby reduced oxidative stress²⁴. SIRT3 directly deacetylated MnSOD and altered the enzymatic activity of MnSOD, and then scavenged mtROS²⁵. Additionally, SIRT3 interacted with forkhead box O3a (FoxO3a) in the

mitochondria, and induced FoxO3a expression to protect cells from oxidative stress and glucose-induced mitochondrial dysfunction in relation to overexpression of MnSOD^{26,27}.

The present study was designed to test a hypothesis that TCEP may provoke cytotoxicity and cell cycle arrest via a ROS-mediated mitochondrial dysfunction pathway in human liver cells.

2. Materials and methods

2.1. Chemicals

TCEP, dimethyl sulfoxide (DMSO), 3-(4, 5-dimethylthiazol-2-yl)-2, 5-diphenyl-tetrazolium bromide (MTT), neutral red, 5,6-Chloromethyl-2,7-dichlorodihydrofluorescein diacetate (CM-H₂DCFDA), RNAase, and propidium iodide (PI) were obtained from Sigma (Sigma-Aldrich Inc., St. Louis, MO, USA). RPMI (Roswell Park Memorial Institute)-1640 medium and fetal bovine serum (FBS) were purchased from GIBCO[®] (Gibco BRL, Gaithersburg, MD, USA). A stock solution of TCEP (4×10^5 mg/L) was made in DMSO, and a neutral red solution (50.00 µg/ml) was made in RPMI 1640 medium (pH6.8). Additionally, a stock solution of MTT (5.00 mg/ml) was prepared in phosphate buffer solution (PBS, pH7.5).

2.2. Cell culture and treatment

Chang liver cells (a human non-malignant liver cell line) were obtained from the Cell Bank of Type Culture Collection of Chinese Academy of Science (Shanghai, China). Cells were grown in RPMI-1640 medium supplemented with 10% FBS at 37°C in a 5% CO₂, 95% air humidified atmosphere. After adherence, cells were treated with the fresh medium

containing TCEP (3.12, 12.50, 50.00 and 200.00 mg/L) or DMSO (as a solvent control, final concentration: < 0.1%). At 24 or 48 h after treatment, cells were harvested for further experiments.

2.3. Cytotoxicity

2.3.1. MTT assay

The MTT assay was used to determine cell viability. Briefly, cells were seeded onto 96-well plates at a density of 5×10^3 cells per well for 18 h, and treated with TCEP at the indicated concentrations. At 24 and 48 h after treatment, cells were washed with PBS (pH7.5) and then incubated with the MTT solution (final concentration, 0.50 mg/ml) for 4 h. The MTT-formazan product was dissolved in 200 μ l of DMSO. The absorbance was measured at 570 nm using a microplate reader (BioTek Instruments Inc., Winooski, Vermont, USA). The cell viability was calculated according to the formula: cell viability (%) =

$$(A570_{\text{treated}} - A570_{\text{blank}}) / (A570_{\text{negative}} - A570_{\text{blank}}) \times 100\%.$$

2.3.2. Neutral red uptake assay

The neutral red uptake assay was also used to assess cell viability. Briefly, cells were seeded onto 96-well plates at a density of 5×10^3 cells per well, and treated with TCEP at the indicated concentrations. At 24 and 48 h after treatment, cells were washed in PBS (pH7.5), incubated with the neutral red solution (50.00 μ g/ml) for 3 h, fixed with the formaldehyde solution (1%, v/v), cultured with elution medium (EtOH/AcOH, 50%/1%, 200 μ l per well), and then followed by gentle shaking for 10 min to achieve a complete dissolution. The absorbance was recorded at 540 nm using a microplate reader (BioTek Instruments Inc., Winooski, Vermont, USA). The absorbance of the control wells was assumed to be 100%,

and the cell viability of the treated wells was determined with respect to the control wells.

The lysosomal integrity (%) = $(A540_{\text{treated}} - A540_{\text{blank}}) / (A540_{\text{negative}} - A540_{\text{blank}}) \times 100\%$.

2.4. Cell cycle analysis

Cell cycle analysis was performed by propidium iodide (PI) staining and flow cytometry²⁸. Briefly, cells were seeded onto 6-well plates at a density of 1×10^5 cells/well for 18 h. After attachment, cells were treated with TCEP at the indicated concentrations. At 24 and 48 h after treatment, cells were harvested and resuspended in 500 μl PBS, fixed in 70% cold alcohol overnight, thereby stained with 10 μl PI (0.5mg/mL) and 5 μl RNase A (1 mg/mL) stock solutions at 37°C in the dark for 1 h. The untreated cells as the negative control were simultaneously measured. Finally, samples were analyzed by flow cytometry (BD Biosciences, Franklin Lakes, NJ, USA). The nuclear DNA (nDNA) distribution was analyzed by ModFit 5.2 software (Verity Software House, Topsham, ME).

2.5. Mitochondrial oxidative stress

2.5.1. Mitochondrial ROS level

The mtROS levels were detected according to the method described earlier²⁹. Briefly, cells were seeded in 90 mm petri dishes at a density of 1×10^6 cells/dish for 18 h, and then treated with TCEP at the indicated concentrations. At 24 and 48 h after treatment, mitochondria were isolated from TCEP-treated cells using a commercial kit from Beyotime institute of biotechnology (Haimen, Jiangsu, China). The mitochondria were suspended in 200 μl of the storage buffer and then incubated with 5-(6)-chloromethyl-2',7'-dichlorodihydrofluorescein diacetate (CM-H₂DCFDA, 10 μM) at 37°C for 20 min. The fluorescence compound 2',7'-dichlorofluorescein (DCF) was measured

immediately using a fluorescence plate reader (BioTek Instruments Inc., Winooski, Vermont, USA) with excitation at 485 nm and emission at 528 nm. Data were normalized to mitochondrial protein concentrations. The concentrations of mitochondrial proteins were determined by the BCA protein assay (Thermo Fisher Scientific Inc., MD, USA).

2.5.2. MnSOD activity

MnSOD activities were measured by a spectrophotometric method. Briefly, cells were seeded onto 6-well plates at a density of 1×10^5 cells/well for 18 h, and then treated with TCEP at the indicated concentrations. At 24 and 48 h after treatment, cells were harvested and employed to measure MnSOD activity using a commercial kit (Nanjing Jiancheng Bioengineering Institute, Nanjing, Jiangsu, China). The MnSOD activity was expressed in units per gram protein.

2.6. Mitochondrial damage and dysfunctions

2.6.1. Mitochondrial membrane potential

Cells were seeded onto 6-well plates at a density of 1×10^5 cells/well for 18 h, and treated then with TCEP at the indicated concentrations. At 24 and 48 h after treatment, cells were harvested and then resuspended in 600 μ l of 5,5',6,6'-tetrachloro-1,1',3,3'-tetraethyl-benzimidazolcarbocyanine iodide (10 μ g/ml, JC-1, Beyotime institute of biotechnology, Haimen, Jiangsu, China), and then incubated at 37°C for 30 min in the dark. The fluorescence value was measured by a FACSort flow cytometer (BD Biosciences, Franklin Lakes, NJ, USA). Data were analyzed by using the cellquest software (BD Biosciences, Franklin Lakes, NJ, USA). The mitochondrial membrane potential (MMP) was expressed as a ratio of percentages of the Q2 (JC-1, PE-A) and Q4 (JC-1, FITC-A).

2.6.2. Mitochondrial DNA copy number

The copy number of mitochondrial DNA (mtDNA) were determined by quantitative PCR³⁰. Briefly, cells were seeded onto 6-well plates at a density of 1×10^5 cells/well for 18 h. After attachment, cells were treated with TCEP at the indicated concentrations. At 24 and 48 h after treatment, cells were harvested and then lysed. nDNA and mtDNA from the cells were isolated using a genomic DNA purification kit (Tiangen Biotech Co.LTD, Beijing, China) and a QIAamp DNA mini kit (Qiagen Sample & Assay Technologies, Shanghai, China), respectively. Quantification of DNA (nDNA and mtDNA) was determined using a NanoDrop ND-100 UV-Vis spectrophotometer (Nanodrop Technologies, Wilmington, DE, USA). mtDNA and nDNA (30 ng each) as the templates were used in the PCR reactions, respectively. The primer sequences for mitochondrial ND1 gene and nuclear gene 18S were as follows: ND1 forward primer: CCCTAAAACCCGCCACATCT; ND1 reverse primer: GAGCGATGGTGAGAGCTAAGGT; 18S forward primer: ACGGACCAGAGCGAAAGCAT; 18S reverse primer: GGACATCTAAGGGCATCACAGAC. The thermal cycling conditions were as follows: at 50°C for 2 min to digest, at 95°C for 5 min to activate the DNA polymerase, followed by 40 cycles at 95°C for 15s to denaturant and at 60°C for 60s to annealing/extension³¹. All PCR-reactions were performed on a 7900HT Fast Real-Time PCR System (Applied Biosystems, Foster City, CA, USA), using SYBR green/ROX qPCR master mix (Thermo Fisher Scientific Co., Ltd, Beijing, China). The raw data obtained from real-time qPCR was analyzed by the comparative C_T ($\Delta\Delta C_T$) method³². The results were expressed as a relative copy number of mtDNA per diploid nDNA.

2.6.3. Cellular ATP Level

Cellular ATP levels were measured by a luciferase-based ATP assay kit (Beyotime institute of biotechnology, Haimen, Jiangsu, China), according to manufacturer's instruction. Briefly, cells were seeded onto 6-well plates at a density of 1×10^5 cells/well for 18 h. After attachment, cells were treated with TCEP at the indicated concentrations. At 24 and 48 h after treatment, cells were harvested and then lysed. Cellular ATP level was measured using a microplate reader (BioTek Instruments Inc., Winooski, Vermont, USA). The ATP level was normalized with the total protein in lysates of the cells and was expressed as micromole per gram total protein.

2.6.4. Intracellular free Ca^{2+} level

Intracellular free Ca^{2+} levels were measured by the reported method³³ with a modification. Briefly, cells were seeded onto 6-well plates at a density of 1×10^5 cells/well for 18 h. After attachment, cells were treated with TCEP at the indicated concentrations. At 24 and 48 h after treatment, cells were harvested, washed and loaded with Fluo3-AM (3 μ M, Beyotime institute of biotechnology, Haimen, Jiangsu, China) for 1 h at 37°C in the dark. The mean fluorescence intensity was detected by a FACSort flow cytometer (BD Biosciences, Franklin Lakes, NJ, USA), with excitation at 488 nm and emission at 525 nm. Data were analyzed by using the CellQuest software (BD Biosciences, Franklin Lakes, NJ, USA).

2.7. SIRT3 transcriptional expression

SIRT3 transcriptional expression was detected by quantitative real-time PCR. Briefly, cells were seeded onto 6-well plates at a density of 1×10^5 cells per well for 18 h. After attachment, cells were treated with TCEP at the indicated concentrations. The harvested cells

were washed three times with PBS (pH7.5), and then used to isolate total RNA by the RNeasy Pure Cell Kit (Qiagen Biotech Co., LTD., Beijing, China). The first strand cDNA was synthesized using the RevertAid First Strand cDNA Synthesis kit (Thermo Fisher Scientific Inc., MD, USA) according to the manufacturer's instructions. The primers were synthesized by Shengon Biotech Co., Ltd. (Shanghai, China). The primer sequences for *SIRT3* and *GAPDH* genes were as follows: forward primer for *SIRT3*: TGGAAACTACAAGCCCAACG, reverse primer for *SIRT3*: ACACTCTCTCAAGCCCATCG; forward primer for *GAPDH*: GAAATCCCATCACCATCTTCCAGG, reverse primer for *GAPDH*: AGCTTCCCGTTCTCAGCCTT. Quantitative real-time PCR was performed using SYBR® Green qPCR SuperMix-UDG kit (Thermo Fisher Scientific Inc., Beijing, China) according to the manufacturer's instruction. Each reaction was consisted of 0.2 µl (10 µM) each of primer, 2 µl of the cDNA product, 5 µl of 2 × SYBR Green PCR Master Mix) and 2.6 µl RNA enzyme-free water. Real-time qPCR reactions were performed on ABI 7900 HT Fast Real Time PCR system (Applied Biosystem, Foster City, CA, USA). RT-PCR conditions were as follows: one cycle at 50°C for 2 min, at 95°C for 5 min, followed by 40 cycles at 95°C for 15 s, and finally at 60°C for 60 s. The raw data from the quantitative real-time PCR was analyzed by the comparative C_T ($\Delta\Delta C_T$) method³².

2.8. Proteins expression

2.8.1 Immunofluorescence staining

SIRT3 protein expression was detected by Immunofluorescence staining. Briefly, cells firstly seeded onto 6-well plates at a density of 1×10^5 cells per well for 18 h, and were

treated with TCEP at the indicated concentrations for 24 and 48 h. The treated-cells were fixed for 15 min with paraformaldehyde (v/v: 4%), permeabilized with Triton-X-100 (v/v: 0.1%) in PBS (pH7.5) at room temperature for 20 min, and blocked with BSA (w/v: 1%) at 37°C for 1 h. Finally, cells were incubated with the primary antibody (rabbit monoclonal anti-SIRT3 antibody, 5 µg/mL) at 4°C overnight, rinsed in PBS (pH7.5) for three times and incubated with goat anti-rabbit Dylight-conjugated secondary antibody (1:5000) at room temperature for 2 h, and the cellular nuclei were counterstained with 1 µg/mL DAPI. The cells were visualized with a confocal scanning laser microscopy system (400 ×, Olympus FV-500, Tokyo, Japan). The images were reconstructed for stereopair images with FLUO-VIEW software (Olympus, Tokyo, Japan) by an independent observer over five individual pictures. The mean fluorescence intensity of SIRT3 expression was analyzed using Image pro-Plus 6.0 software (Olympus, Tokyo, Japan). The expression of SIRT3 protein were expressed as the mean of fluorescence density.

2.8.2 Western blotting

The protein expression of SIRT3, FoxO3a and MnSOD was detected by western blotting. Briefly, cells were seeded in 60 mm petri dish at a density of 4×10^5 cells/dish for 18 h. After attachment, cells were treated with TCEP at the indicated concentrations. At 24 and 48 h after treatment, cells were harvested and lysed in the lysis buffer containing 1 mM phenylmethylsulfonyl fluoride (Beyotime institute of biotechnology, Haimen, Jiangsu, China). Each sample (30-40 µg) was loaded and electrophoresed on 10% SDS–polyacrylamide gels. The resolved proteins were transferred to polyvinylidene fluoride membranes (Pall Corporation, NY, USA). The membrane was incubated with the appropriate primary antibody,

including anti-SIRT3 antibody (1:500, abcam[®], Cambridge, MA, USA), anti-FoxO3a antibody, anti-MnSOD antibody (1:500, Bioworld Technology, Inc., Nanjing, China) and anti-GAPDH antibody (1:5000, Bioworld Technology, Inc., Nanjing, China) in blocking buffer (5% dried non-fat milk in Tris-buffered saline) at 4°C overnight. Membranes were then incubated with the appropriate horseradish peroxidase-conjugated goat anti-rabbit IgG HRP-conjugated secondary antibody (1:5000, Bioworld technology, Inc., Nanjing, China) at room temperature for 2 h, and then the reaction was detected with a Gene Gnome imaging system (Syngene Inc., Frederick, MD, USA). The relative densities of the protein bands were analyzed using the Gene tool software (Syngene Inc., Frederick, MD, USA).

2.9. Statistical Analysis

All data were processed with SPSS 12.0 for Windows (SPSS Inc., Chicago, IL, USA). Data were presented as means \pm SD. The statistical significance of differences was determined by one-way analysis of variance (ANOVA), followed by Dunnett's multiple comparison post hoc test or Student's t tests. A value of $p < 0.05$ was considered statistically significant.

3. Results

3.1. TCEP-induced hepatotoxicity

The results from MTT assay showed that at 24 and 48 h after treatment, TCEP reduced the cell viability in a dose-dependent manner ($*p < 0.05$ or $\#p < 0.01$, Fig. 1A); similar results from the neutral red uptake assay were observed ($*p < 0.05$ or $\#p < 0.01$, Fig. 1B).

3.2. TCEP-induced cell cycle arrest

To identify effects of TCEP on cell cycle arrest, cellular DNA content was detected by PI. Cell cycles were arrested at G2/M phase in the 3.12 and 50.00 mg/L TCEP groups at 24 h (* $p < 0.05$ for both, Fig. 2A), and in all TCEP-treated groups at 48 h (* $p < 0.05$ or # $p < 0.01$, Fig. 2B).

3.3. TCEP-induced mitochondrial oxidative stress

To evaluate mitochondrial oxidative stress status in cells, the mtROS levels and MnSOD activities were detected. At 24 and 48 h after treatment, increased mtROS levels were found in the 50.00 and 200.00 mg/L TCEP-treated groups (* $p < 0.05$ or # $p < 0.01$, Fig. 3A). The MnSOD activity was reduced only in the 200.00 mg/L TCEP group at 24 h, and in all TCEP-treated groups at 48 h (* $p < 0.05$ or # $p < 0.01$, Fig. 3B). The reduction of MnSOD activities might partially cause the increase of mtROS production.

3.4. TCEP-induced mitochondrial dysfunctions

To determine whether TCEP affected mitochondrial function and integrity, we measured changes in MMP, mtDNA copy number, ATP level and intracellular free Ca²⁺ concentration. TCEP decreased MMP in all TCEP-treated groups at 24 h, but only in the 200.00 mg/L TCEP group at 48 h (* $p < 0.05$ or # $p < 0.01$, Figs. 4). TCEP reduced relative mtDNA copy number in all TCEP-treated groups at 24 and 48 h (* $p < 0.05$ or # $p < 0.01$, Fig. 5), in a dose-independent manner. TCEP decreased intracellular ATP levels in all TCEP-treated groups at 24 h, but only in the 200.00 mg/L TCEP group at 48 h (* $p < 0.05$, Fig. 6). TCEP increased intracellular free Ca²⁺ concentrations in the 50.00 and 200.00 mg/L TCEP groups at 24 and 48 h (# $p < 0.01$ for all, Figs. 7A-C).

3.5. Regulators involved in TCEP-induced mitochondrial dysfunction

Results from the RT-PCR and immunofluorescence staining showed that TCEP down-regulated the expression of SIRT3 at both mRNA and protein levels at 24 and 48 h after treatment (* $p < 0.05$ or # $p < 0.01$, Figs. 8A-C). Results from the western blotting indicated that TCEP down-regulated the expression of FoxO3a protein in all TCEP-treated groups, and of SIRT3 protein in the > 3.12 mg/L TCEP groups, as well as of MnSOD protein only in the 200.00 mg/L TCEP group at 24 and 48 h after treatment (* $p < 0.05$ or # $p < 0.01$, Figs. 9A-C).

4. Discussion

Previous studies have shown that TCEP is widely distributed in the environment including household dust (0-7605 ng/g), surface water (92-2620 ng/L), and drinking water (0-26.2 ng/L) samples³⁴⁻³⁶. Average levels of occupational exposure to TCEP (such as uses of TCEP in producing polymers and formulations) varied from 420 mg/person/day to 2500 mg/person/day⁷. TCEP was also detected in human biological samples, such as human breast milk (ranging from 0.14 to 42 ng/g lipid weight) and human hair (maximum concentration: 1950 ng/g dry weight)^{5,6}. Moreover, TCEP at the concentrations ranging between 10 μ g/L and 2500 mg/L was used for *in vitro* studies on cytotoxicity^{37,38}. Thus, based on the results of previous studies and our own preliminary experiments, TCEP with a range from 3.12 to 200.00 mg/L was used in this study.

Chang liver cells were isolated from non-malignant human liver tissue. They are often used to create an *in vitro* model to investigate the liver toxicities of chemicals. In the present study, TCEP markedly reduced the cell viability at the concentrations of > 3.12 mg/L.

Several studies reported that TCEP reduced cell viabilities of PC12 cells at the concentrations $\geq 40 \mu\text{M}$ (equal to 11.42 mg/L)³⁹ and of primary cultured rabbit renal proximal tubule cells at the concentrations $\geq 10.00 \text{ mg/L}$ ³⁸. Thus, the results implied that Chang liver cells may be more sensitive to TCEP-induced toxicity than either PC12 cells or primary cultured rabbit renal proximal tubule cells.

Mitochondrial oxidative stress is an early event. *In vitro* studies showed that mitochondrial oxidative stress caused decreases in the MMP and mtDNA copy number; and increased the cytoplasmic free Ca^{2+} levels and reduced ATP synthesis, and ultimately lead to mitochondrial dysfunction^{40,41}. Chen et al. recently reported that TCEP could induce oxidative stress in TM3 cells⁴². We found that TCEP induced the mitochondrial oxidative stress (Fig. 3), disrupted mitochondrial integrity (Figs. 4 and 5), and led to mitochondrial dysfunctions (Figs. 6 and 7), indicating that there was a linkage between mtROS and intercellular calcium deregulation or reduced ATP synthesis in TCEP-treated Chang liver cells.

Mitochondria contain large numbers of key molecules that regulate cell survival, death, metabolic pathways. Therefore, mitochondrial dysfunction can cause cell cycle arrest, senescence and apoptosis^{19,43-45}. SIRT3 is a critical regulator for maintaining mitochondrial integrity and function by modulating oxidative stress pathways. SIRT3 deacetylates certain metabolic and respiratory enzymes (such as MnSOD) to prevent excessive accumulation of mtROS^{46,47}. Whereas, SIRT3 overexpression antagonized oxidative stress in human diploid fibroblasts⁴⁸. We observed that TCEP downregulated SIRT3 and MnSOD proteins, decreased MnSOD enzymatic activity, and then attenuated scavenging of mtROS, led to

mitochondrial oxidative stress. Studies reported that knockout SIRT3 caused mitochondrial or cellular ROS in mouse embryonic fibroblasts⁴⁶, while SIRT3-FOXO3a-MnSOD signaling was involved in mitochondrial oxidative stress⁴⁹. SIRT3 directly deacetylated MnSOD and altered MnSOD enzymatic activity⁵⁰. The results showed that TCEP induced mitochondrial oxidative stress, mitochondrial dysfunction, and ultimately led to G2/M cell cycle arrest in Chang liver cell, accompanied by attenuating the scavenging of mtROS in Chang liver cells.

The above results indicated that TCEP may induce cell cycle arrest in Chang liver cells through SIRT3 down-regulation and a ROS-mediated mitochondrial dysfunction pathway.

Conflict of Interest

The authors declare that there are no conflicts of interest.

Funding

This work was financially supported by the National Natural Science Foundation of China (Grant No.81273023).

References

1. A. Araki, I. Saito, A. Kanazawa, K. Morimoto, K. Nakayama, E. Shibata, M. Tanaka, T. Takigawa, T. Yoshimura and H. Chikara, *Indoor Air*, 2014, **24**, 3-15.
2. S. Esteban, M. Gorga, M. Petrovic, S. González-Alonso, D. Barceló and Y. Valcárcel, *Sci. Total Environ.*, 2014, **466**, 939-951.
3. A. Bradman, R. Castorina, F. Gaspar, M. Nishioka, M. Colón, W. Weathers, P. P. Egeghy, R. Maddalena, J. Williams and P. L. Jenkins, *Chemosphere*, 2014, DOI:

- 10.1016/j.chemosphere.2014.02.072.
4. H. M. Stapleton, J. Misenheimer, K. Hoffman and T. F. Webster, *Chemosphere*, 2014, DOI: 10.1016/j.chemosphere.2013.12.100.
 5. L. Y. Liu, A. Salamova, K. He and R. A. Hites, *J Chromatogr A*, 2015, **1406**, 251-257.
 6. J.-W. Kim, T. Isobe, M. Muto, N. M. Tue, K. Katsura, G. Malarvannan, A. Sudaryanto, K.-H. Chang, M. Prudente and P. H. Viet, *Chemosphere*, 2014, DOI: 10.1016/j.chemosphere.2014.02.033.
 7. *EU Risk Assessment Report, Tris (2-chloroethyl) phosphate, TCEP*, European Commission, Dortmund, 2009.
 8. D. Chapman, S. Michener and G. Powis, *Toxicol Sci*, 1991, **17**, 215-224.
 9. L. Burka, J. Sanders, D. Herr and H. Matthews, *Drug Metab Dispos*, 1991, **19**, 443-447.
 10. M. Beth-Hübner, *Int Arch Occ Env Hea*, 1999, **72**, M017-M023.
 11. H. Matthews, S. Eustis and J. Haseman, *Toxicol Sci*, 1993, **20**, 477-485.
 12. P. Schumacker, *Cancer Cell*, 2015, **27**, 156-157.
 13. K. N. Papanicolaou, G. A. Ngoh, E. R. Dabkowski, K. A. O'Connell, R. F. Ribeiro, W. C. Stanley and K. Walsh, *Am Jo Physiol-Heart C*, 2012, **302**, 167-179.
 14. X. Li, P. Fang, J. Mai, E. T. Choi, H. Wang and X. F. Yang, *J Hematol Oncol*, 2013, **6**, 1-19.
 15. S. W. Tait and D. R. Green, *J Cell Sci*, 2012, **125**, 807-815.
 16. D. Pessayre, A. Berson, B. Fromenty and A. Mansouri, *Semin Liver Dis*, 2000, **21**, 57-69.
 17. P. Venditti, L. Di Stefano and S. Di Meo, *Mitochondrion*, 2013, **13**, 71-82.
 18. W. Zhang, Y. Liu, Z. An, D. Huang, Y. Qi and Y. Zhang, *Toxicol In Vitro*, 2011, **25**,

- 979-984.
19. P. S. Brookes, Y. Yoon, J. L. Robotham, M. Anders and S.-S. Sheu, *Am J Physiol Cell Physiol*, 2004, **287**, 817-833.
20. M. Chang, Y. Ho, P. Lee, C. Chan, J. Lee, L. Hahn, Y. Wang and J. Jeng, *Carcinogenesis*, 2001, **22**, 1527-1535.
21. M. D. Hirschey, T. Shimazu, E. Goetzman, E. Jing, B. Schwer, D. B. Lombard, C. A. Grueter, C. Harris, S. Biddinger and O. R. Ilkayeva, *Nature*, 2010, **464**, 121-125.
22. B. H. Ahn, H. S. Kim, S. Song, I. H. Lee, J. Liu, A. Vassilopoulos, C. X. Deng and T. Finkel, *P Nat Acad Sci*, 2008, **105**, 14447-14452.
23. A. Giralt and F. Villarroya, *Biochem J*, 2012, **444**, 1-10.
24. K. Brown, S. Xie, X. Qiu, M. Mohrin, J. Shin, Y. Liu, D. Zhang, D. T. Scadden and D. Chen, *Cell Rep.*, 2013, **3**, 319-327.
25. Y. Chen, J. Zhang, Y. Lin, Q. Lei, K. L. Guan, S. Zhao and Y. Xiong, *EMBO Rep*, 2011, **12**, 534-541.
26. S. Munusamy and L. A. MacMillan-Crow, *Free Radical Bio Med*, 2009, **46**, 1149-1157.
27. K. E. Boyle, S. A. Newsom, R. C. Janssen, M. Lappas and J. E. Friedman, *J Clin Endocr Mrtab*, 2013, **98**, 1601-1609.
28. P. Pozarowski and Z. Darzynkiewicz, in *Checkpoint Controls and Cancer*, Springer, 2004, pp. 301-311.
29. M. Degli Esposti, *Methods*, 2002, **26**, 335-340.
30. S. E. Hunter, D. Jung, R. T. Di Giulio and J. N. Meyer, *Methods*, 2010, **51**, 444-451.
31. N. Pieters, G. Koppen, K. Smeets, D. Napierska, M. Plusquin, S. De Prins, H. Van De

- Weghe, V. Nelen, B. Cox and A. Cuypers, *PloS One*, 2013, **8**, e63208.
32. T. D. Schmittgen and K. J. Livak, *Nat Protoc*, 2008, **3**, 1101-1108.
33. P. A. Vandenberghe and J. L. Ceuppens, *J Immunol Methods*, 1990, **127**, 197-205.
34. N. Ali, A. C. Dirtu, N. V. d. Eede, E. Goosey, S. Harrad, H. Neels, A. t Mannetje, J. Coakley, J. Douwes and A. Covaci, *Chemosphere*, 2012, **88**, 1276-1282.
35. S. D. Kim, J. Cho, I. S. Kim, B. J. Vanderford and S. A. Snyder, *Water Res*, 2007, **41**, 1013-1021.
36. L. P. Padhye, H. Yao, F. T. Kung'u and C.-H. Huang, *Water Res*, 2014, **51**, 266-276.
37. W. Föllmann and J. Wober, *Toxicol Lett*, 2006, **161**, 124-134.
38. X. Ren, Y. J. Lee, H. J. Han and I. S. Kim, *Chemosphere*, 2008, **74**, 84-88.
39. N. Ta, C. Li, Y. Fang, H. Liu, B. Lin, H. Jin, L. Tian, H. Zhang, W. Zhang and Z. Xi, *Toxico Lett*, 2014, **227**, 164-171.
40. C. S. Liu, C. S. Tsai, C. L. Kuo, H. W. Chen, C. K. Lii, Y. S. Ma and Y. H. Wei, *Free Radical Res*, 2003, **37**, 1307-1317.
41. L. Liu, J. R. Trimarchi and D. L. Keefe, *Biol Reprod*, 2000, **62**, 1745-1753.
42. G. Chen, S. Zhang, Y. Jin, Y. Wu, L. Liu, H. Qian and Z. Fu, *Reprod Toxicol*, 2015, **57**, 100-110.
43. Y. S. Yoon, H. O. Byun, H. Cho, B. K. Kim and G. Yoon, *J Biol Chem*, 2003, **278**, 51577-51586.
44. H. Nakahara, T. Kanno, Y. Inai, K. Utsumi, M. Hiramatsu, A. Mori and L. Packer, *Free Radical Bio Med*, 1998, **24**, 85-92.
45. A. Gholami, R. Kassis, E. Real, D. S. Guadagnini, M. C. Prevost, Y. Jacob, F. Larrous

- and D. Obach, *J Virol*, 2008, **82**, 4774–4784.
46. H. S. Kim, K. Patel, K. Muldoon Jacobs, K. S. Bisht, N. Aykin Burns, J. D. Pennington, R. van der Meer, P. Nguyen, J. Savage and K. M. Owens, *Cancer Cell*, 2010, **17**, 41-52.
47. A. S. Bause and M. C. Haigis, *Exp Gerontol*, 2013, **48**, 634-639.
48. B. Zhang, S. Cui, X. Bai, L. Zhuo, X. Sun, Q. Hong, B. Fu, J. Wang, X. Chen and G. Cai, *Age*, 2013, **35**, 2237-2253.
49. J. D. Pennington, K. M. Jacobs, M. V. Mishra, P. Nguyen and D. Gius, *Mitochondrion*, 2007, **7**, 423.
50. R. Tao, A. Vassilopoulos, L. Parisiadou, Y. Yan and D. Gius, *Antioxid Redox Sign*, 2014, **20**, 1646-1654.

Figure legends

Fig. 1. Cytotoxicity of TCEP-treated Chang liver cells. Cells were treated with TCEP (3.12, 12.50, 50.00 and 200.00 mg/L) for 24 and 48 h. DMSO diluted in RPMI-1640 medium was used as the solvent control (final concentration: < 0.1%). Cell viability was measured by either the MTT assay (A) or the neutral red staining method (B). Cell viability of TCEP-treated cells was expressed as a percentage of untreated cells. Results are representative of at least three independent experiments (mean \pm SD). The relative absorbance values of the controls from three independent experiments were obtained from the MTT assay and neutral red cell viability assay, and assumed to be 100%. The symbols denote statistically significant differences compared with the control group: * p < 0.05, # p < 0.01.

Fig. 2. Effects of TCEP on cell cycle arrest in Chang liver cells. Cells were treated with TCEP (3.12, 12.50, 50.00 and 200.00 mg/L) for 24 (A) and 48 h (B). DMSO diluted in RPMI-1640 medium was used as the solvent control (final concentration: < 0.1%). Cell cycles in TCEP-treated cells were detected by flow cytometry. The cell cycle distribution is expressed as the percent of the total cells in each phase by dividing the number of cells in a given phase. Results are represented by the mean \pm SD of three individual experiments. The symbols denote statistically significant differences compared with the control group: * p < 0.05, # p < 0.01.

Fig. 3. Effects of TCEP on mitochondrial oxidative stress in Chang liver cells. Cells were treated with TCEP (3.12, 12.50, 50.00 and 200.00 mg/L) for 24 and 48 h. DMSO diluted in

RPMI-1640 medium was used as the solvent control (final concentration: < 0.1%). (A) Levels of mtROS formation in TCEP-treated cells were measured by a fluorescence spectroscopy method. (B) Cellular manganese superoxide dismutase (MnSOD) activities were assessed using a MnSOD assay kit. The MnSOD activity is expressed as units per gram protein. Results are represented by the mean \pm SD of three individual experiments. The symbols denote statistically significant differences compared with the control group: * p < 0.05, # p < 0.01.

Fig. 4. Effects of TCEP on mitochondrial membrane potential in Chang liver cells. Cells were treated with TCEP (3.12, 12.50, 50.00 and 200.00 mg/L) for 24 and 48 h. DMSO diluted in RPMI-1640 medium was used as the solvent control (final concentration: < 0.1%). Mitochondrial membrane potentials (MMP) in TCEP-treated cells were assayed by flow cytometry. (A) Representative quadrant plots for each treatment. (B) The bar chart of MMP. The MMP is expressed as a ratio of the percentage of cells in Q2 and the percentage of cells in Q4. Results are represented by the mean \pm SD of three individual experiments. The symbols denote statistically significant differences compared with the control group: * p < 0.05, # p < 0.01.

Fig. 5. Effects of TCEP on mitochondrial DNA copy number in Chang liver cells. Cells were treated with TCEP (3.12, 12.50, 50.00 and 200.00 mg/L) for 24 and 48 h. DMSO (< 0.1%) in RPMI-1640 medium was used as the solvent control. Mitochondrial DNA (mtDNA) copy numbers in TCEP-treated cells were determined by a quantitative real-time PCR. The

mitochondrial copy number is expressed as a relative copy number of mtDNA per diploid nDNA. Results are represented by the mean \pm SD of three individual experiments. The C_T values of the controls from three independent experiments were obtained from real time PCR, and assumed to be 1.00. The symbols denote statistically significant differences compared with the control group: * $p < 0.05$, # $p < 0.01$.

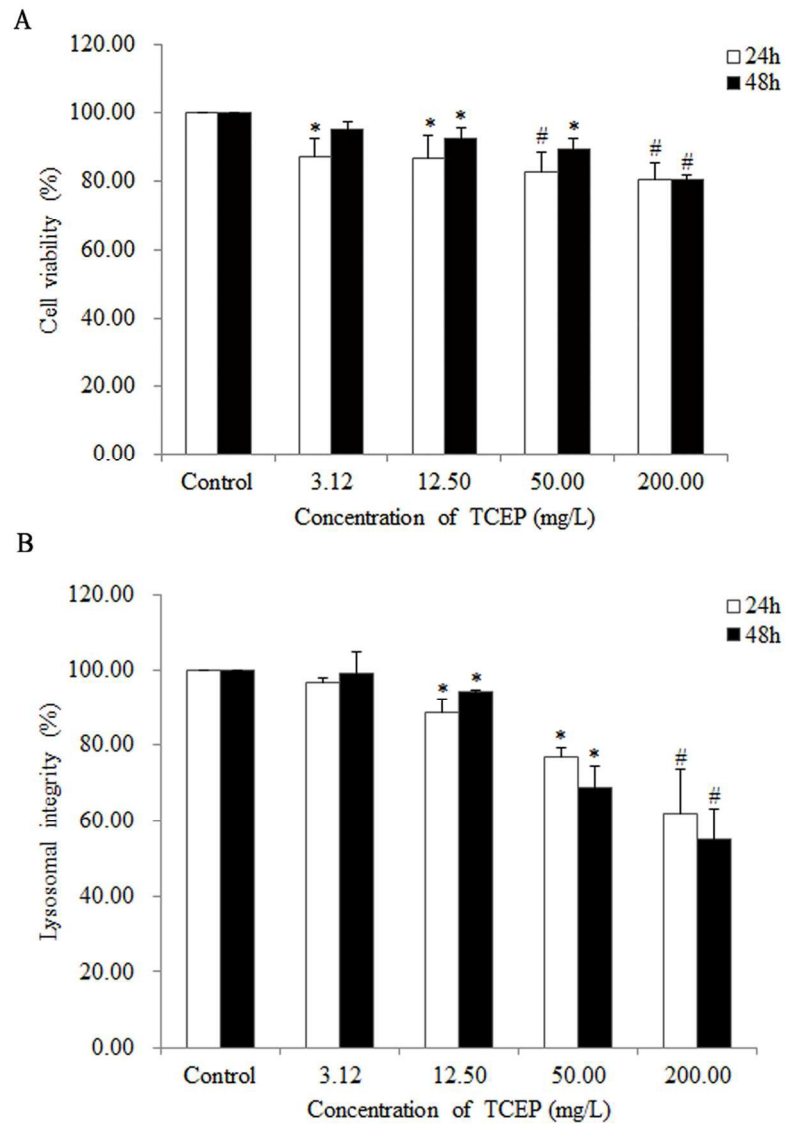
Fig. 6. Effects of TCEP on mitochondrial ATP synthesis in Chang liver cells. Cells were treated with TCEP (3.12, 12.50, 50.00 and 200.00 mg/L) for 24 and 48 h. DMSO diluted in RPMI-1640 medium was used as the solvent control (final concentration: $< 0.1\%$). Intracellular ATP levels in TCEP-treated cells were measured using ATP assay kit (Beyotime institute of biotechnology, Haimen, Jiangsu, China). The ATP level is expressed as micromole per gram protein. Results are represented by the mean \pm SD of three individual experiments. The symbols denote statistically significant differences compared with the control group: * $p < 0.05$, # $p < 0.01$.

Fig. 7. Effects of TCEP on the intracellular free Ca^{2+} levels in Chang liver cells. Cells were treated with TCEP (3.12, 12.50, 50.00 and 200.00 mg/L) for 24 and 48 h. DMSO diluted in RPMI-1640 medium was used as the solvent control (final concentration: $< 0.1\%$). The intracellular free Ca^{2+} levels in TCEP-treated cells were assayed by flow cytometry. (A) Representative single parameter histogram plots for each treatment. (B) Representative composite diagram by Photoshop software for each treatment. (C) The bar chart of intracellular free Ca^{2+} levels. The intracellular free Ca^{2+} level is expressed as mean

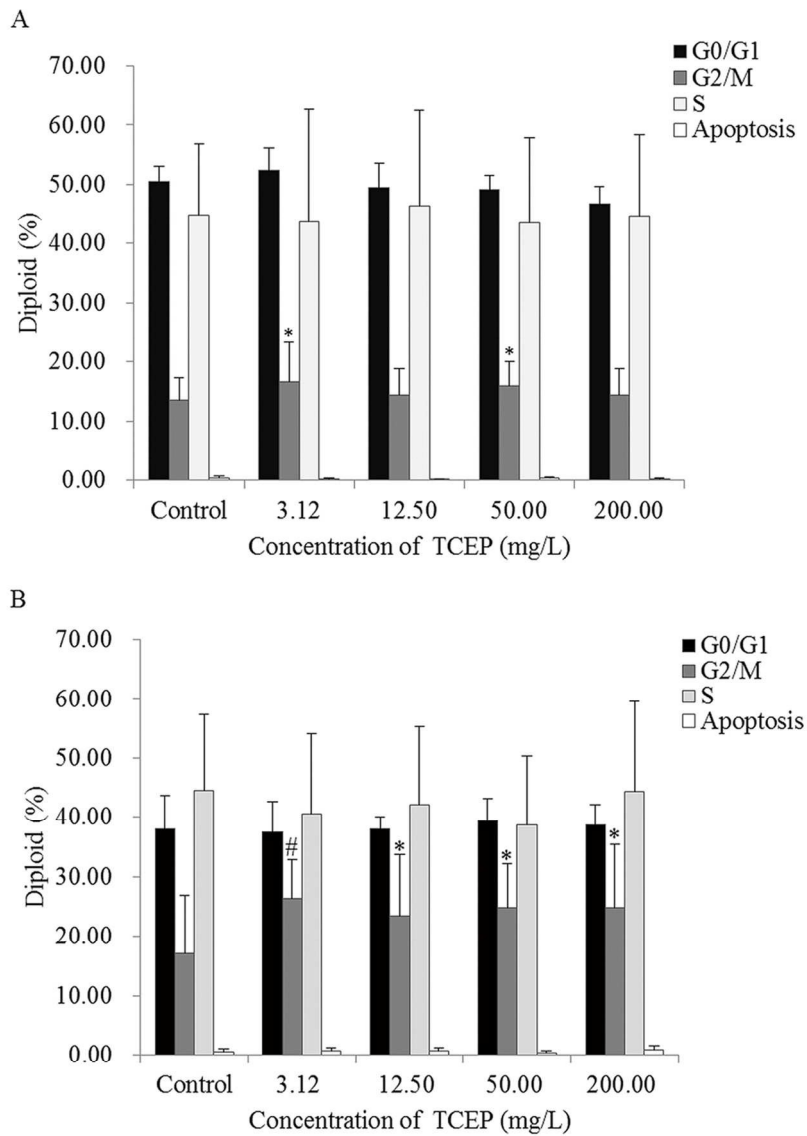
fluorescence intensity of Fluo-3. Results are represented by the mean \pm SD of three individual experiments. The symbols denote statistically significant differences compared with the control group: # $p < 0.01$.

Fig. 8. Effects of TCEP on the expression of SIRT3 mRNA and protein in Chang liver cells. Cells were treated with TCEP (3.12, 12.50, 50.00 and 200.00 mg/L) for 24 and 48 h, respectively. DMSO diluted in RPMI-1640 medium was used as the solvent control (final concentration: $< 0.1\%$). (A) The expression of SIRT3 mRNA in TCEP-treated cells were detected by real time PCR. (B) The expression of SIRT3 protein in TCEP-treated cells were detected by immunofluorescence. (C) The bar chart of SIRT3 mean density. Results are represented by the mean \pm SD of three individual experiments. The symbols denote statistically significant differences compared with the control group: * $p < 0.05$, # $p < 0.01$.

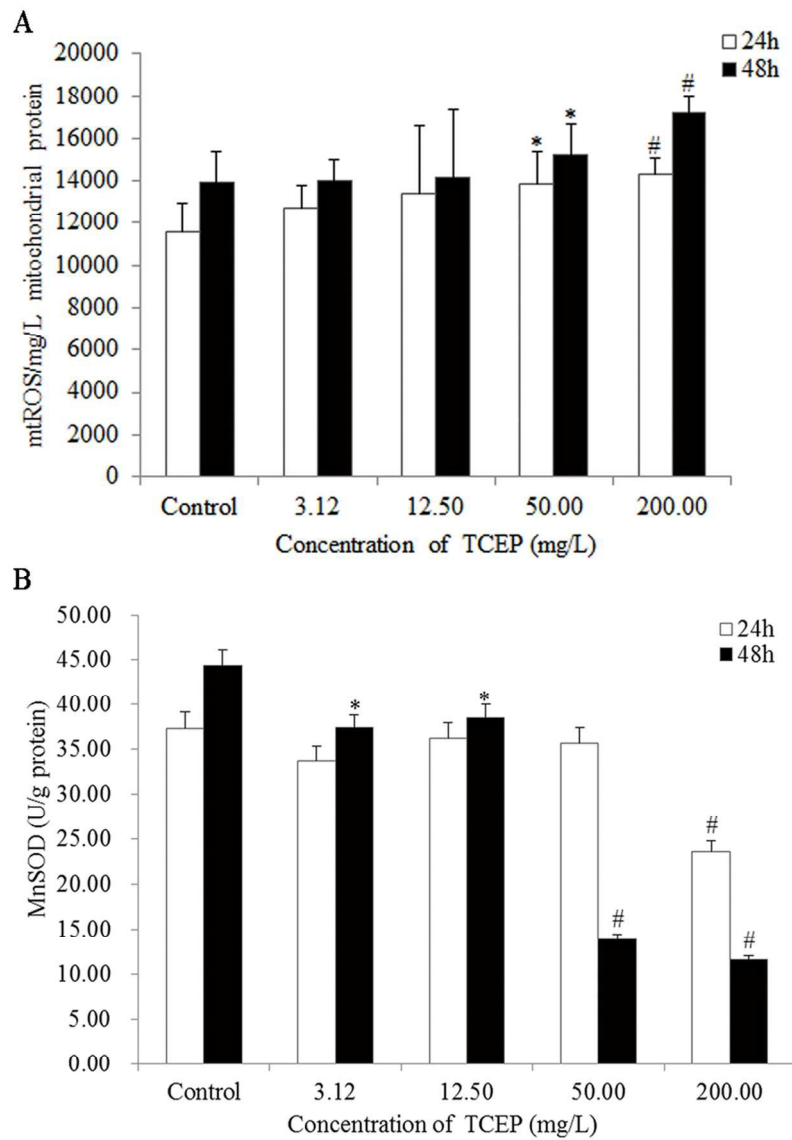
Fig. 9. Effects of TCEP on the expression of regulatory proteins (FoxO3a, SIRT3 and MnSOD) in Chang liver cells. Cells were treated with TCEP (3.12, 12.50, 50.00 and 200.00 mg/L) for 24 (A) and 48 h (B), respectively. DMSO ($< 0.1\%$) in RPMI-1640 medium was used as the solvent control. The expression of the studied proteins was analyzed by Western blotting. (C) The bar chart of the relative expression of proteins. Results are represented by the mean \pm SD of three individual experiments. The symbols denote statistically significant differences compared with the control group: * $p < 0.05$, # $p < 0.01$.



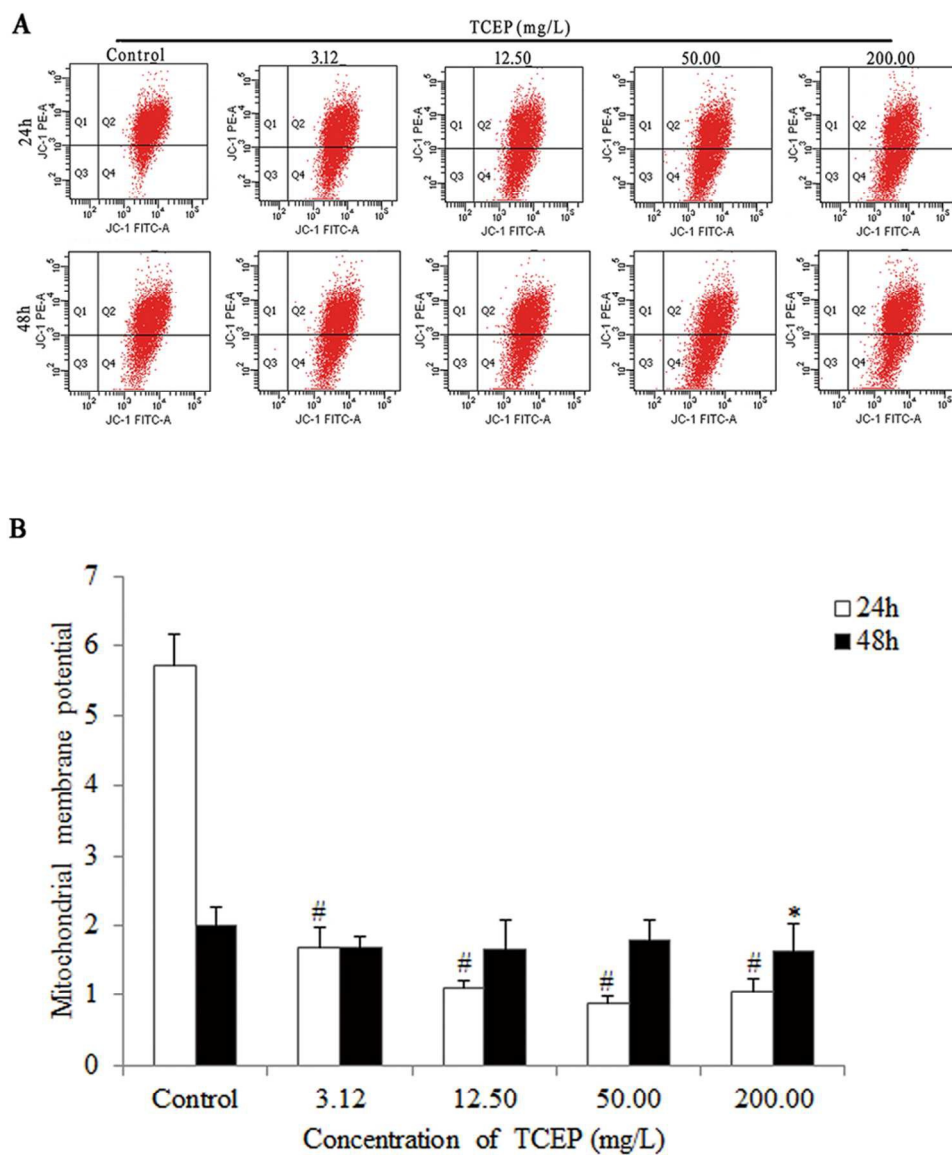
Cytotoxicity of TCEP-treated Chang liver cells.
125x176mm (300 x 300 DPI)



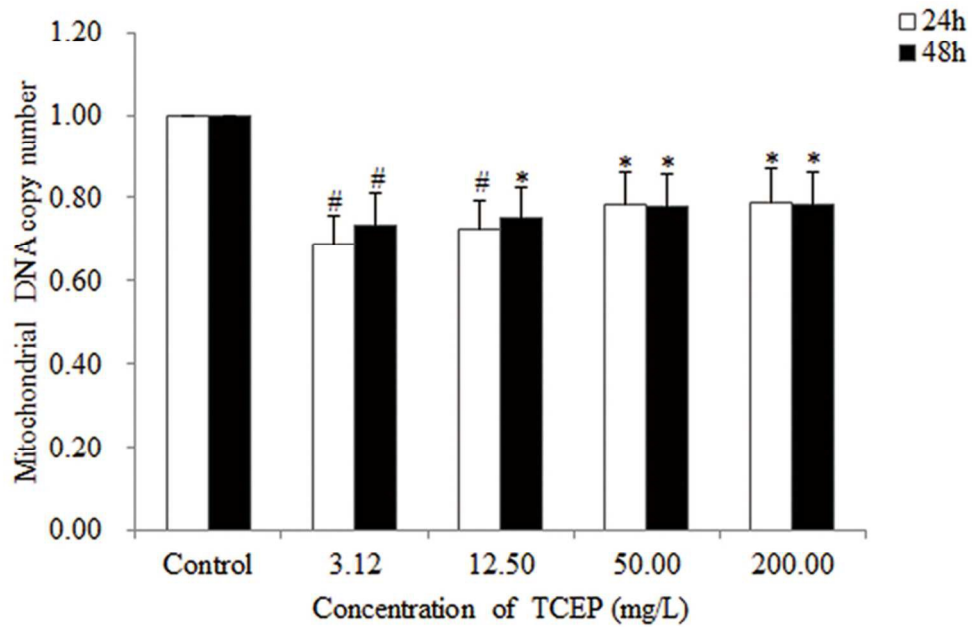
Effects of TCEP on cell cycle arrest in Chang liver cells.
126x181mm (300 x 300 DPI)



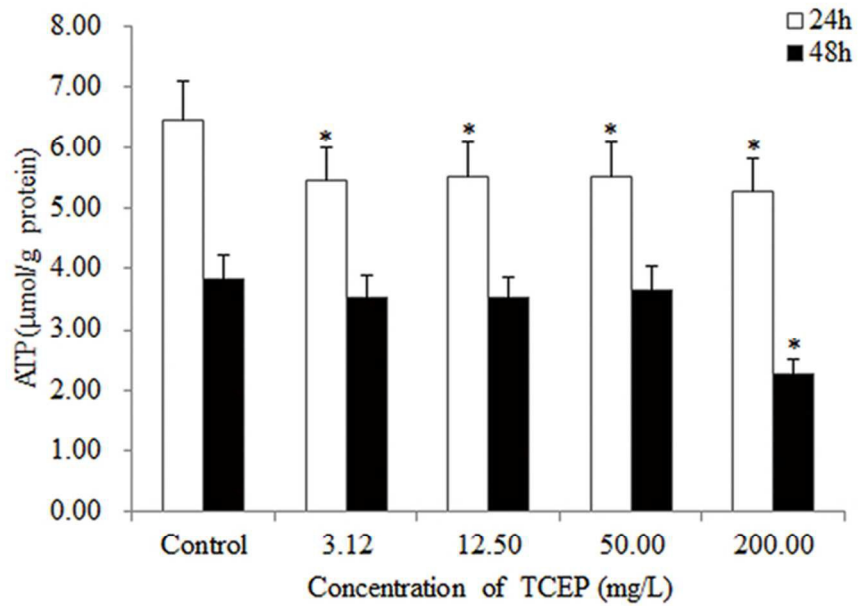
Effects of TCEP on mitochondrial oxidative stress in Chang liver cells.
124x174mm (300 x 300 DPI)



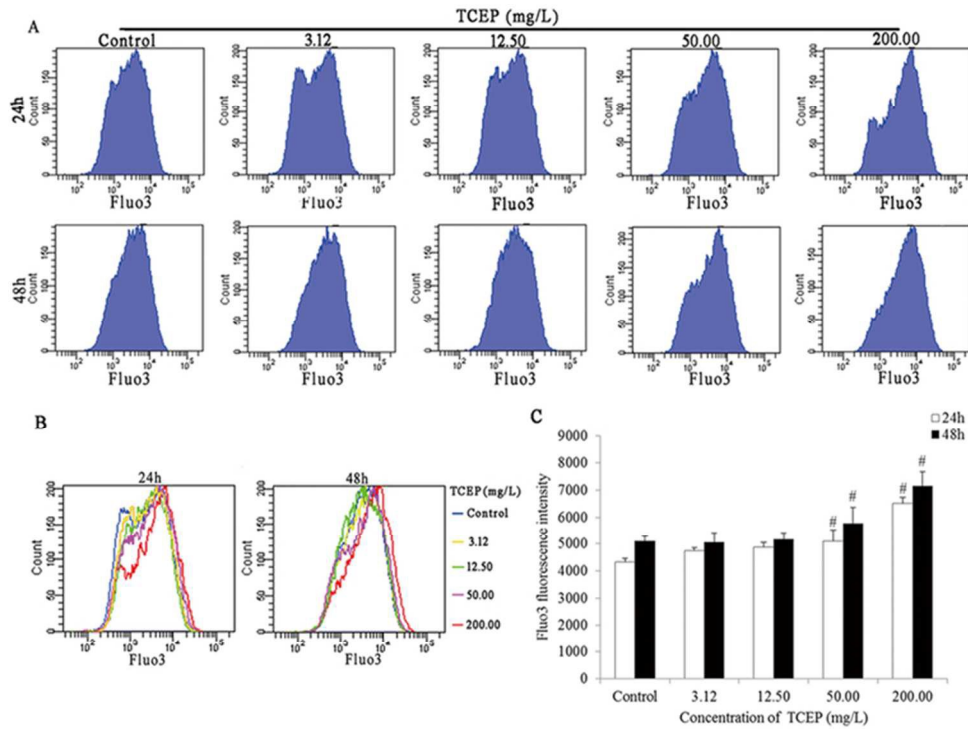
Effects of TCEP on mitochondrial membrane potential in Chang liver cells.
88x106mm (300 x 300 DPI)



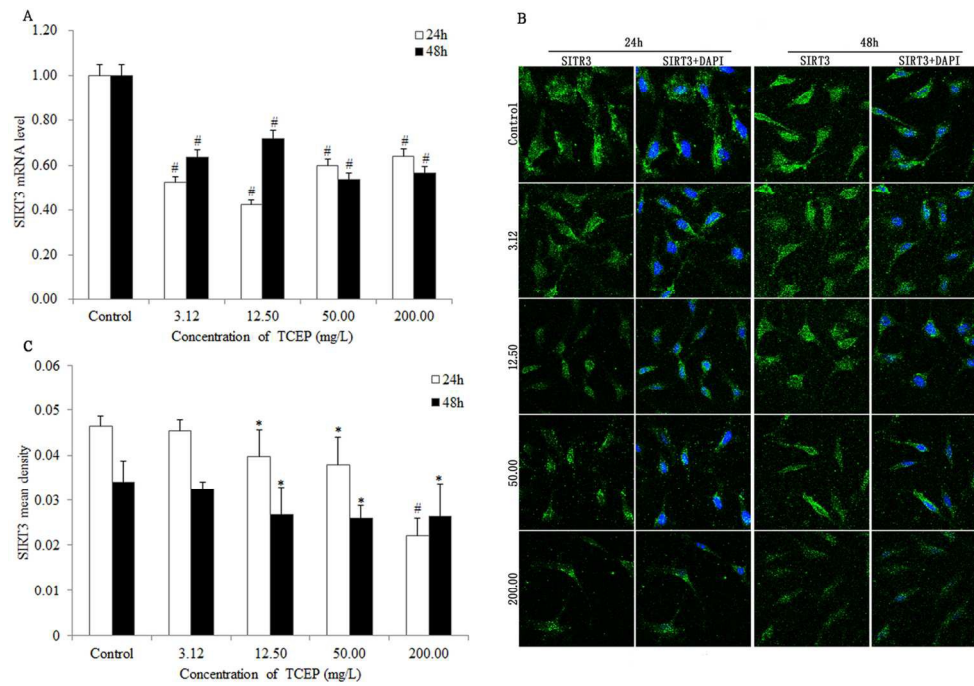
Effects of TCEP on mitochondrial DNA copy number in Chang liver cells.
63x45mm (300 x 300 DPI)



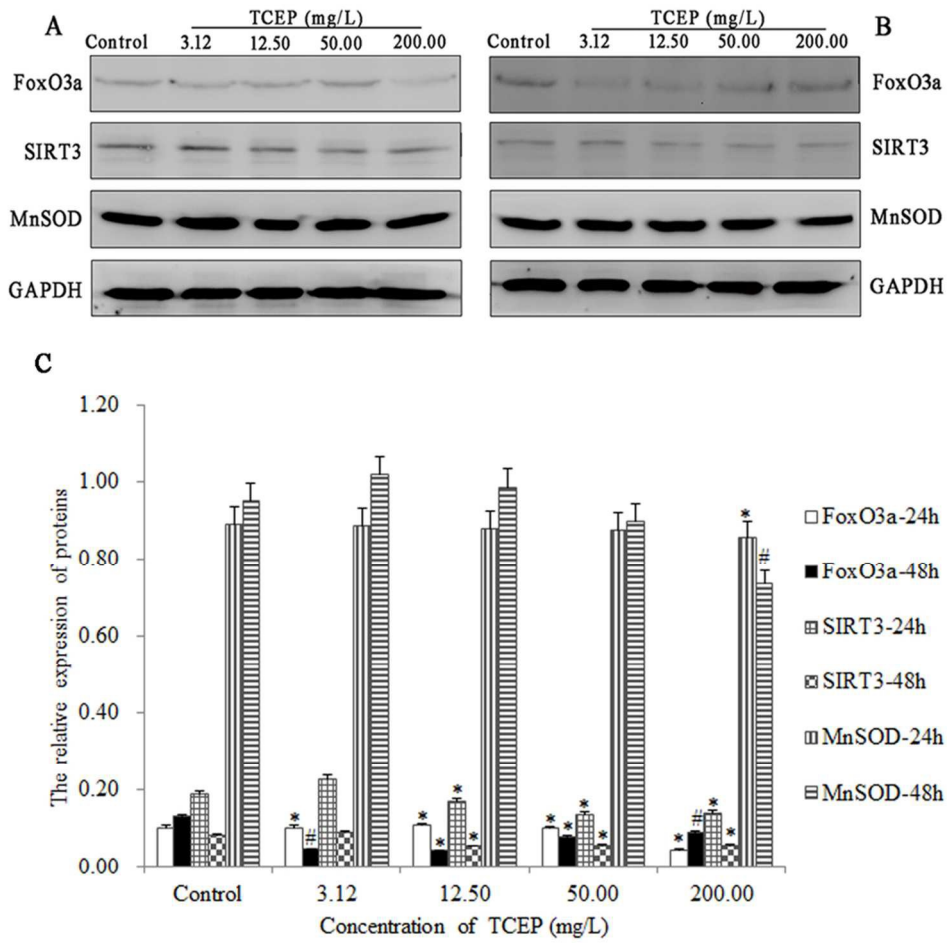
Effects of TCEP on mitochondrial ATP synthesis in Chang liver cells.
61x42mm (300 x 300 DPI)



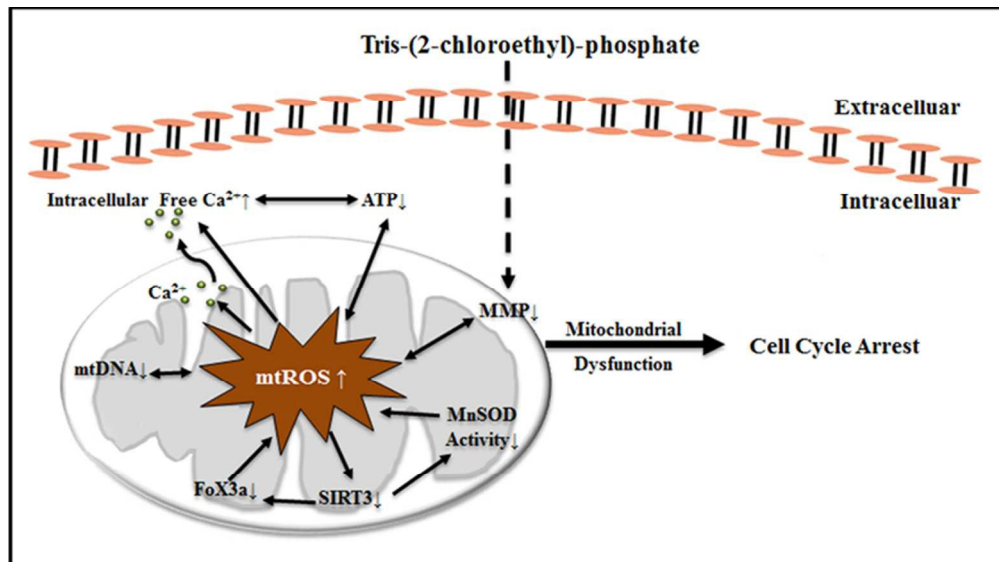
Effects of TCEP on the intracellular free Ca^{2+} levels in Chang liver cells.
66x49mm (300 x 300 DPI)



Effects of TCEP on the expression of SIRT3 mRNA and protein in Chang liver cells.
124x86mm (300 x 300 DPI)



Effects of TCEP on the expression of regulatory proteins (FoxO3a, SIRT3 and MnSOD) in Chang liver cells. 90x90mm (300 x 300 DPI)



71x39mm (300 x 300 DPI)